Liquid Crystals
Publication details, including instructions for authors and subscription information:
http://www.informaworld.com/smpp/title~content=t713926090

Flow and reorientation in the dynamics of nematic defects

André M. Sonnet[a]; Epifanio G. Virga[b]
[a] Department of Mathematics, University of Strathclyde, Scotland, UK [b] Dipartimento di Matematica and CNISM, Università di Pavia, Pavia, Italy

First published on: 22 July 2009

To cite this Article Sonnet, André M. and Virga, Epifanio G.(2009) 'Flow and reorientation in the dynamics of nematic defects', Liquid Crystals, 36: 10, 1185 — 1192, First published on: 22 July 2009 (iFirst)
To link to this Article: DOI: 10.1080/02678290903034480
URL: http://dx.doi.org/10.1080/02678290903034480

Liquid Crystals,
Vol. 36, Nos. 10–11, October–November 2009, 1185–1192

Taylor & Francis
Taylor & Francis Group

INVITED ARTICLE

Flow and reorientation in the dynamics of nematic defects

André M. Sonnet[a] and Epifanio G. Virga[b]*

[a]*Department of Mathematics, University of Strathclyde, Livingstone Tower, 26 Richmond Street, Glasgow G1 1XH, Scotland, UK;* [b]*Dipartimento di Matematica and CNISM, Università di Pavia, Via Ferrata 1, 27100 Pavia, Italy.*

(Received 27 March 2009; final form 9 May 2009)

We propose a simple phenomenological model for hydrodynamic defect dynamics in nematic liquid crystals, inspired by the Ericksen–Leslie theory. We identify the main forces that govern both fluid and defect motion and we comment on their symmetry. As shown for two annihilating disclinations, our model is predictive for arbitrary length scales and topological charges.

Keywords: nematic liquid crystals; defect dynamics; disclinations; Ericksen–Leslie equations

1. Introduction

Topological defects and their dynamics play an important role in liquid crystals. Here, in particular, we are concerned with nematic liquid crystals for which defect dynamics is easily accessible experimentally, as typical timescales are very convenient and boundary conditions can be well controlled. From the theoretical side, the Ericksen–Leslie equations that govern the hydrodynamics of nematic liquid crystals are well established (*1*, *2*): they couple the flow field $\mathbf{v}$ and the evolution of the nematic director $\mathbf{n}$.

In a nematic liquid crystal, the motion of a defect can have two different origins: material transport of the defect due to fluid flow and displacement due to director reorientation. For problems without external sources of flow, most workers in the past have neglected flow effects and considered only the reorientational dynamics. A common assumption was that backflow, that is, the flow induced by reorientation, would merely lead to a reduction in the rotational viscosity, thereby effectively speeding up the reorientation process. The importance and the role of backflow in defect dynamics has already been appreciated in (*3*), and it has received more attention in (*4–6*). Experimental evidence for an asymmetry in the motion of annihilating defect pairs cannot be explained with pure reorientational dynamics (*7–9*).

However, the presence of defects leads to severe problems in Ericksen–Leslie's equations. The director field at a defect is undefined and divergences in the free energy and dissipation densities usually require a cut-off at the defect core. Numerical schemes fail because of discretisation errors due to diverging gradients at the defects. The numerical works presented in (*4–6*) have therefore resorted to a Landau model that avoids singularities but introduces a natural length scale, the nematic coherence length. On present-day computers, this limits the applicability to sample sizes in the micrometre range, but it can reasonably be expected that similar results would hold also for larger defect distances. This conjecture has not yet been shown to stand on firm ground.

Here we pursue a different approach. We propose a model for defect dynamics in nematic liquid crystals that includes backflow. It is valid when the director reorientation is the *source* of fluid flow. Our analysis is based on the Ericksen–Leslie equations and hence there is no principle restriction on the size of the domain. We treat the problem associated with divergences at the defects in a way that is similar to that used in statics and reorientational dynamics, i.e. by introducing a suitable cut-off where necessary. The reorientation dynamics is treated as if it were unaffected by the backflow. For the flow itself, we assume that there is a neighbourhood of the defect in which the fluid moves with homogeneous velocity. The apparent velocity $\dot{\mathbf{x}}$ of the defect is then $\dot{\mathbf{x}} = \mathbf{v} + \mathbf{u}$, where $\mathbf{v}$ is the instantaneous velocity of the fluid at the defect and $\mathbf{u}$ is the velocity of the defect that is due to reorientation.

The paper is organised as follows. In Section 2, we identify the forces acting on a moving defect, of either elastic and dissipative origins. In Section 3, we compute these forces for a model problem, where two line disclinations with opposite topological charges move towards each other. In Section 4, we draw conclusions from the analysis of this example which are likely to be valid in general.

*Corresponding author. Email: eg.virga@unipv.it

ISSN 0267-8292 print/ISSN 1366-5855 online

DOI: 10.1080/02678290903034480
http://www.informaworld.com

2. Forces on a nematic defect

In this section, we present our approximate phenomenological model for the dynamics of a nematic defect. The model is based on the balance of all forces acting on the defect.

2.1 Ericksen–Leslie equations

Ericksen–Leslie theory can be formulated conveniently in terms of a free energy $W(\mathbf{n}, \nabla\mathbf{n})$ per unit volume and a Rayleigh dissipation function R,

$$R = \frac{1}{2}\gamma_1 \overset{\circ}{\mathbf{n}}{}^2 + \gamma_2 \overset{\circ}{\mathbf{n}} \cdot \mathbf{D}\mathbf{n} + \frac{1}{2}\gamma_3 (\mathbf{D}\mathbf{n})^2 + \frac{1}{2}\gamma_4 \operatorname{tr} \mathbf{D}^2 + \frac{1}{2}\gamma_5 (\mathbf{n} \cdot \mathbf{D}\mathbf{n})^2, \tag{1}$$

where the γ_i ($i = 1, \ldots, 5$) are viscosity coefficients, $\mathbf{D}$ is the symmetric part of the velocity gradient, and $\overset{\circ}{\mathbf{n}}$ is the co-rotational derivative of the nematic director $\mathbf{n}$. The equations of motion then take the form (*10*)

$$\frac{\partial R}{\partial \overset{\circ}{\mathbf{n}}} = \operatorname{div} \frac{\partial W}{\partial \nabla \mathbf{n}} - \frac{\partial W}{\partial \mathbf{n}} + \lambda \mathbf{n} \tag{2}$$

and

$$\rho \dot{\mathbf{v}} = \operatorname{div} \mathbf{T}, \tag{3}$$

where λ is a Lagrange multiplier and

$$\mathbf{T} = -p\mathbf{I} + \mathbf{T}^{(\mathrm{e})} + \mathbf{T}^{(\mathrm{v})} \tag{4}$$

is the stress tensor. Here p is the hydrostatic pressure, to be determined so as to make the flow isochoric,

$$\operatorname{div} \mathbf{v} = 0. \tag{5}$$

Moreover,

$$\mathbf{T}^{(\mathrm{e})} := W\mathbf{I} - (\nabla \mathbf{n})^{\mathrm{T}} \frac{\partial W}{\partial \nabla \mathbf{n}} \tag{6}$$

is Ericksen's elastic stress (*11*, *12*), and

$$\mathbf{T}^{(\mathrm{v})} := \frac{1}{2}\left(\mathbf{n} \otimes \frac{\partial R}{\partial \overset{\circ}{\mathbf{n}}} - \frac{\partial R}{\partial \overset{\circ}{\mathbf{n}}} \otimes \mathbf{n} \right) + \frac{\partial R}{\partial \mathbf{D}} \tag{7}$$

is the viscous stress.

2.2 Phenomenological model for defect dynamics

Rather than attempting the daunting task of finding an exact analytical solution to Equations (2), (3) and (5), we use these equations as guidance to assess the dynamics of defect motion. To start, we make the approximation that the reorientation process does *not* depend on the flow. This seems reasonable as long as the flow is a secondary phenomenon that is caused by the reorientation. Then, the reorientation velocity $\mathbf{u}$ can be determined in the usual way by considering Equation (2) only.

To assess the flow velocity at the defect, we imagine that there is a neighbourhood $\mathcal{B}$ of the defect that moves with velocity $\mathbf{v}$ due to material flow, and we consider the balance of forces on $\mathcal{B}$. Care has to be taken because the divergence theorem is not applicable to regions that contain defects. Hence, forces on a region $\mathcal{B}$ that contains a defect cannot be determined by Equation (3), but the traction $\mathbf{T}\boldsymbol{\nu}$ has to be integrated on $\partial\mathcal{B}$, where $\boldsymbol{\nu}$ is the unit outer normal to $\partial\mathcal{B}$. While this might seem slightly counterintuitive, it actually makes the notion of a *force on a defect* meaningful. Take, for example, the equilibrium director field of a pair of defects at a fixed distance. The divergence of the elastic stress (6) vanishes for static solutions of (2), but still the integral of the traction yields a non-zero force on each defect (*12*). Moreover, this force is the same on any contour that contains just a single defect, and so it should indeed be interpreted as a force on the defect.

We regard the stress tensor as the sum of three parts,

$$\mathbf{T} = \mathbf{T}^{(\mathrm{e})} + \mathbf{T}^{(\mathrm{r})} + \mathbf{T}^{(\mathrm{d})}, \tag{8}$$

where $\mathbf{T}^{(\mathrm{e})}$ is the elastic stress as above,

$$\mathbf{T}^{(\mathrm{r})} := \frac{1}{2}\gamma_1 (\mathbf{n} \otimes \overset{\circ}{\mathbf{n}} - \overset{\circ}{\mathbf{n}} \otimes \mathbf{n}) \tag{9}$$

is the part of the viscous stress that is caused by reorientation in the absence of flow, and $\mathbf{T}^{(\mathrm{d})}$ is the remaining part of the stress including also the hydrostatic pressure. $\mathbf{T}^{(\mathrm{d})}$ stems from terms in the dissipation that are proportional to the stretching $\mathbf{D}$.

The forces

$$\mathbf{f}^{(\mathrm{e})} := \int_{\partial\mathcal{B}} \mathbf{T}^{(\mathrm{e})} \boldsymbol{\nu} \, \mathrm{d}A \tag{10}$$

and

$$\mathbf{f}^{(\mathrm{r})} := \int_{\partial\mathcal{B}} \mathbf{T}^{(\mathrm{r})} \boldsymbol{\nu} \, \mathrm{d}A \tag{11}$$

depend on the director field and the reorientation process, in particular $\mathbf{f}^{(\mathrm{r})} \propto \mathbf{u}$. Since $\mathbf{T}^{(\mathrm{d})}$ depends in

an intricate way on the flow field, knowledge of a full solution to Equations (2), (3) and (5) would be required to compute the force

$$\mathbf{f}^{(\mathrm{d})} := \int_{\partial\mathcal{B}} \mathbf{T}^{(\mathrm{d})}\boldsymbol{\nu}\,\mathrm{d}A \tag{12}$$

exactly. Here, we assume that it gives rise to a *drag force* on the defect that opposes the *material* motion of the defect,

$$\mathbf{f}^{(\mathrm{d})} = -\mu\mathbf{v}. \tag{13}$$

We regard μ as a phenomenological constant that may depend, for example, on the topological charge of the defect and details of the geometry, such as the distance between annihilating defects.

To summarise, when inertia is neglected, the following balance equation is satisfied along the flow

$$\mathbf{f}^{(\mathrm{e})} + \mathbf{f}^{(\mathrm{r})} + \mathbf{f}^{(\mathrm{d})} = \mathbf{0}, \tag{14}$$

where $\mathbf{f}^{(\mathrm{e})}$ depends only on the director distortion, while

$$\mathbf{f}^{(\mathrm{r})} \propto \mathbf{u} \quad \text{and} \quad \mathbf{f}^{(\mathrm{d})} \propto -\mathbf{v}. \tag{15}$$

This allows one to determine $\mathbf{v}$ and then $\dot{\mathbf{x}} = \mathbf{u} + \mathbf{v}$ gives the defect velocity.

2.3 *Symmetry and parity*

In defect annihilation, further knowledge can be gained on the forces $\mathbf{f}^{(\mathrm{e})}$ and $\mathbf{f}^{(\mathrm{r})}$ acting on the two defects, as they enjoy specific symmetry properties. We consider a pair of defects of opposite topological charge that lie on a common symmetry axis $\mathbf{e}$. Then all forces are along this axis. Further symmetry properties arise if the director field $\mathbf{n}^{+}$ around one defect can be mapped into that around the other $\mathbf{n}^{-}$, by means of the parity transformation

$$\mathbf{n}^{-} = \mathbf{R}\mathbf{n}^{+}, \tag{16}$$

where

$$\mathbf{R} = \mathbf{I} - 2\mathbf{e} \otimes \mathbf{e} \tag{17}$$

is the reflection about the plane orthogonal to $\mathbf{e}$. It can easily be deduced from Equations (9) and (11) that

$$\mathbf{f}^{(\mathrm{r})-} = \mathbf{f}^{(\mathrm{r})+}, \tag{18}$$

whereas, in the one elastic constant approximation, it follows from Equation (10) that

$$\mathbf{f}^{(\mathrm{e})-} = -\mathbf{f}^{(\mathrm{e})+}. \tag{19}$$

This means that the elastic forces will accelerate both defects towards each other, while the reorientational viscous forces will speed up one of the defects and slow down the other.

3. Disclination annihilation

While the concepts outlined above are fairly general and may be applicable to different classes of materials, they are best illustrated by example. To this end, we consider the annihilation of a pair of straight disclination lines with opposite topological charges s and $-s$. For disclinations in the z-direction, the director can be written as

$$\mathbf{n} = \cos\varphi\,\mathbf{e}_x + \sin\varphi\,\mathbf{e}_y. \tag{20}$$

We assume that the evolution is described in the *near-field* limit so that the orientation pattern for any defect distance minimises the elastic free energy, which we take in the one-constant approximation. Then, if the two disclinations intersect the (x, y)-plane at $(x = \pm a,\ y = 0)$, φ takes the explicit form (see, e.g., (*13*))

$$\varphi = s\arctan\frac{2ay}{x^2 + y^2 - a^2}, \tag{21}$$

where $a = a(t)$. Equation (21) is a good approximation to the dynamical director field close to the defects. Further away, the solution given in (*14*), and also used in (*15*), should be employed instead.

To assess the reorientation dynamics, we neglect flow and make use of the dissipation equality that states that

$$\dot{\mathcal{F}} + \mathcal{D} = 0, \tag{22}$$

where $\dot{\mathcal{F}}$ is the rate of change of the free energy in a cylindrical region $\mathcal{B}$ of unit height traversed by both disclinations and $\mathcal{D} = \int_{\mathcal{B}} 2R\,\mathrm{d}A$ is the total energy dissipated in $\mathcal{B}$ (see (*16*, *17*)). From (1) and (21) the Rayleigh dissipation function is

$$R = \frac{1}{2}\gamma_1 \left(\frac{\partial \varphi}{\partial a}\dot{a}\right)^2, \tag{23}$$

and the free energy density is

$$W = \frac{1}{2}K|\nabla \mathbf{n}|^2 = \frac{1}{2}K|\nabla \varphi|^2. \tag{24}$$

With φ given by (21), we obtain from (23) and (24) that

$$R = \frac{2\gamma_1 s^2 y^2 (x^2+y^2+a^2)^2 \dot{a}^2}{[x^4+y^4+a^4+2(x^2y^2+a^2y^2-a^2x^2)]^2} \tag{25}$$

and

$$W = \frac{2Ka^2s^2}{x^4+y^4+a^4+2(x^2y^2+a^2y^2-a^2x^2)}. \tag{26}$$

We integrate these densities in the infinite strip $-\infty < x < \infty$, $-L < y < L$, excluding a small strip $-r_c < y < r_c$, where r_c is a defect core radius, see Figure 1.

We interpret L as a cut-off length, delimiting the region within which the defect annihilation takes place: we expect the far fields of the two annihilating defects to cancel each other outside this region, although our simplified model is unable to capture such a feature completely. Improving on (*14*), Denniston proved in (*15*) that with an appropriately computed far field, the annihilation time is independent of the cut-off length. For simplicity, we have renounced following Denniston's approach, and consequently, in our model, the annihilation time will exhibit a dependence on the cut-off length. However, we do not regard this as a severe shortcoming, because differences in the far fields are only significant for asymptotically free defects. In our context, the defects become asymptotically free only in the final stages of their annihilation, and so the overall effect of misrepresenting the far field is small. We thus arrive at

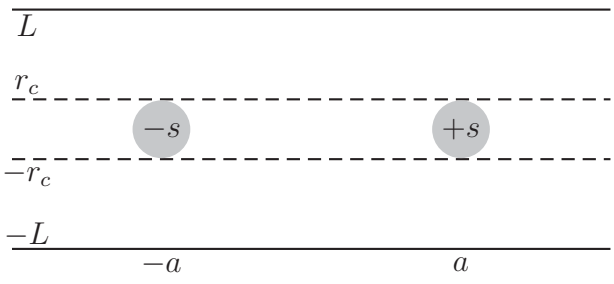

Figure 1. Domain of integration.

$$\mathcal{D} = \pi\gamma_1 s^2 \dot{a}^2 \ln \frac{L^2(L^2+a^2)}{r_c^2(r_c^2+a^2)} \tag{27}$$

and

$$\mathcal{F} = \pi K s^2 \ln \frac{L^2(r_c^2+a^2)}{r_c^2(L^2+a^2)}. \tag{28}$$

With (27) and (28), the dissipation equality then becomes a differential equation for $a(t)$:

$$\frac{2K}{\gamma_1}\frac{L^2-r_c^2}{(a^2+r_c^2)(a^2+L^2)} + \ln\frac{L^2(a^2+L^2)}{r_c^2(a^2+r_c^2)}\frac{\dot{a}}{a} = 0. \tag{29}$$

This equation does not contain s: the reorientation dynamics is independent of the topological charge. Equation (29) allows us to write the speed of the reorientation as a function of the instantaneous value of a, which is half the defect distance $d = 2a$. Under the assumption that $a, L \gg r_c$ and setting

$$\tau := \frac{\gamma_1 L^2}{4K}, \tag{30}$$

we find that

$$\dot{a} = \frac{L^4}{2\tau \ln(a^2r_c^2/L^2(a^2+L^2))a(a^2+L^2)} < 0. \tag{31}$$

This equation allows us to estimate the time T to annihilation in terms of the initial separation between the disclinations and the other geometrical parameters. Letting

$$\alpha := \frac{a^2}{L^2} \quad \text{and} \quad \epsilon := \frac{r_c^2}{L^2}, \tag{32}$$

we give (31) the form

$$\frac{1}{\tau}\frac{1}{1+\alpha} + \ln\left(\frac{1+\alpha}{\epsilon\alpha}\right)\dot{\alpha} = 0. \tag{33}$$

Separation of variables together with requiring that $\alpha(0) = 0$ gives

$$\int_0^{\alpha_i} (1+\alpha)\ln\frac{1+\alpha}{\epsilon\alpha}\,\mathrm{d}\alpha = \frac{T}{\tau}, \tag{34}$$

where α_i is the value of α at the start of the annihilation process. Carrying out the integration in (34) yields

$$-\frac{T}{\tau} = \left(\frac{1}{2}\alpha_i^2 + \alpha_i\right)\ln\epsilon - \frac{1}{2}\left[(2\alpha_i+\alpha_i^2)\ln\left(\frac{1+\alpha_i}{\alpha_i}\right) + \alpha_i + \ln(1+\alpha_i)\right]. \tag{35}$$

Since $\epsilon \ll \alpha_i \ll 1$, a good approximation to (35) is

$$\frac{T}{\tau} \approx -\alpha_i \ln\epsilon, \tag{36}$$

which, by (30), gives

$$T \approx -\frac{\gamma_1 a_i^2}{2K}\ln\frac{r_c}{L}, \tag{37}$$

where a_i is the value of a at the start of the annihilation process. This estimate shows how T only moderately depends on the cut-off length L, a conclusion which *a posteriori* justifies the approximations made to arrive at (37).

3.1 Elastic force

To assess the effects of material flow, we first consider the disclination at $x = a$ and require that the balance of forces (14) hold on a circular contour of radius r_e centred at the disclination, where r_e is an effective defect radius that is not necessarily the same as the core radius r_c.

In polar coordinates (r,ϑ) centred at $x = a$, $y = 0$, the director field $\mathbf{n}$ can be represented as

$$\mathbf{n} = \cos\psi\,\mathbf{e}_r + \sin\psi\,\mathbf{e}_\vartheta, \tag{38}$$

where $\psi := \varphi - \vartheta$. Since $x = a + r\cos\vartheta$ and $y = r\sin\vartheta$, it follows from (21) that

$$\psi = (s-1)\vartheta - s\arctan\frac{r\sin\vartheta}{r\cos\vartheta + 2a}. \tag{39}$$

In general, for any function $\psi = \psi(r,\vartheta)$, we readily obtain from (24) and (6) that

$$W = \frac{K}{2}\left[\psi_{,r}^2 + \frac{1}{r^2}(1+\psi_{,\vartheta})^2\right], \tag{40}$$

where a comma denotes differentiation, and

$$\mathbf{T}^{(\mathrm{e})} = \frac{K}{2}\left[\psi_{,r}^2 + \frac{1}{r^2}(1+\psi_{,\vartheta})^2\right]\mathbf{I} - K\left[\psi_{,r}^2\,\mathbf{e}_r\otimes\mathbf{e}_r + \frac{1}{r}\psi_{,r}(1+\psi_{,\vartheta})(\mathbf{e}_r\otimes\mathbf{e}_\vartheta + \mathbf{e}_\vartheta\otimes\mathbf{e}_r) + \frac{1}{r^2}(1+\psi_{,\vartheta})^2\,\mathbf{e}_\vartheta\otimes\mathbf{e}_\vartheta\right]. \tag{41}$$

By symmetry of the director field, all forces are along the x-axis, and it suffices to compute the x-component of $\mathbf{f}^{(\mathrm{e})}$, which, by (10), is given by

$$\begin{aligned} f^{(\mathrm{e})} &= \mathbf{e}_x\cdot r_e\int_0^{2\pi}\mathbf{T}^{(\mathrm{e})}\mathbf{e}_r\,\mathrm{d}\vartheta \\ &= Kr_e\int_0^{2\pi}\left\{\frac{1}{2}\left[\frac{1}{r_e^2}(1+\psi_{,\vartheta})^2 - \psi_{,r}^2\right]_{r=r_e}\cos\vartheta + \frac{1}{r_e}\left[\psi_{,r}(1+\psi_{,\vartheta})\right]_{r=r_e}\sin\vartheta\right\}\mathrm{d}\vartheta. \end{aligned} \tag{42}$$

By inserting (39) into (42) we obtain that

$$f^{(\mathrm{e})} = \begin{cases} -\frac{\pi K s^2}{a} & \text{for } r_e < 2a, \\ 0 & \text{for } r_e > 2a. \end{cases} \tag{43}$$

3.2 Reorientational viscous force

To compute the reorientational viscous force, we assume that the disclination at $x = a$ moves due to reorientation with a speed $u > 0$ in the negative x-direction. In (20), as in (38), a is a parameter varying with time. In our model, the flow is induced by reorientation; we thus assume that the co-rotational derivative $\mathring{\mathbf{n}}$ coincides with the partial time derivative $\mathbf{n}_{,t}$ of $\mathbf{n}$. Representing $\mathbf{n}$ as in (38), we readily obtain that

$$\mathring{\mathbf{n}} = \varphi_{,t}\mathbf{n}^\perp = \frac{\partial\varphi}{\partial a}\dot{a}\mathbf{n}^\perp, \tag{44}$$

where

$$\mathbf{n}^\perp = -\sin\psi\,\mathbf{e}_r + \cos\psi\,\mathbf{e}_\vartheta. \tag{45}$$

By (9) and (11), we then arrive at

$$\begin{aligned} f^{(\mathrm{r})} &= \mathbf{e}_x \cdot r_e \int_0^{2\pi} \mathbf{T}^{(\mathrm{r})} \mathbf{e}_r \, \mathrm{d}\vartheta \\ &= \frac{1}{2}\gamma_1 \dot{a} r_e \int_0^{2\pi} \frac{\partial \varphi}{\partial a} \Big[(\mathbf{n} \cdot \mathbf{e}_x)(\mathbf{n}^\perp \cdot \mathbf{e}_r) \\ &\quad - (\mathbf{n}^\perp \cdot \mathbf{e}_x)(\mathbf{n} \cdot \mathbf{e}_r) \Big] \mathrm{d}\vartheta \\ &= -\frac{1}{2}\gamma_1 u r_e \int_0^{2\pi} \frac{\partial \varphi}{\partial a} \sin\vartheta \, \mathrm{d}\vartheta, \end{aligned} \tag{46}$$

where we have set $u = -\dot{a}$, since the disclination at $x = a$ is being considered. To compute $\partial\varphi/\partial a$ in (46), we first make use of (21) and then in the result convert the variables x and y into r and ϑ; this yields

$$\frac{\partial \varphi}{\partial a} = \frac{2s}{r} \frac{(2ar\cos\vartheta + 2a^2 + r^2)\sin\vartheta}{4ar\cos\vartheta + 4a^2 + r^2}. \tag{47}$$

Hence, we finally arrive at

$$f^{(\mathrm{r})} = \begin{cases} -\frac{1}{2}\gamma_1 \pi s u \left(1 + \frac{1}{4}\frac{r_e^2}{a^2}\right) & \text{for } r_e \le 2a, \\ -\gamma_1 \pi s u & \text{for } r_e \ge 2a. \end{cases} \tag{48}$$

Thus for $r_e > 2a$, when the contour contains both defects, $f^{(\mathrm{r})}$ is independent of r_e. This can be interpreted as minus the force that the liquid crystal exerts on its container due to the annihilation process. In the case that is relevant for the force balance, $r_e < 2a$, we can approximate $f^{(\mathrm{r})}$ as $-(\pi\gamma_1 s u/2)$, which is independent of r_e.

3.3 *Viscous drag force*

To model the viscous drag force, we depict the core of the disclination as a body submerged in the liquid crystal. Its *material* motion through the surrounding fluid would then be hampered by a resistive force of hydrodynamic nature. To this end, we regard the core as a cylindrical region that is instantaneously centred on the disclination axis and whose material motion is independent of the director reorientation. This view is coherent with regarding the disclination core as consisting of molecules in the isotropic phase. Molecules peripheral to the core will in general partake of phase transitions induced by reorientational motion of the disclination, while molecules in the centre will be merely conveyed by material flow. We regard the viscous drag force as acting on the instantaneous configuration of the core, and so as depending only on the material flow around the disclination produced by its own motion, as if the defect were gliding undistorted.

We recall the force on a cylinder in a Stokes flow (*18*, p. 615),

$$f^{(\mathrm{d})} = -2\pi A \gamma_{\mathrm{eff}} v, \tag{49}$$

where v is the velocity of the cylinder relative to the fluid, γ_{eff} is an effective viscosity, and $A = 2/\ln(7.4/\mathrm{Re})$. It depends weakly on the Reynolds number $\mathrm{Re} = 2r_e\rho U/\gamma_{\mathrm{eff}}$, where U is a typical flow velocity.

In our context, we approximate the resistive force experienced by the disclination as

$$f^{(\mathrm{d})} = -\mu v \tag{50}$$

with a constant μ, where v is now the velocity of the material that instantaneously constitutes the disclination core. The constant μ can in principle be obtained, e.g., from numerical solutions computed on a specific length scale, such as those presented in (*4*, *5*).

To gain information of the dependence of μ on the topological charge s, we look at the backflow that is created by the moving disclination. When a disclination of winding number s passes a given point, the director in that location has to rotate by $s\pi$. Therefore, we expect that the gradient of the induced flow will be proportional to s, and hence that the dissipation associated with it will be proportional to s^2. Thus, the higher the winding number, the stronger the associated drag force.

However, this simple argument does not distinguish between $+s$ and $-s$ defects. A better estimate can be obtained from the incipient flow that would be created by a defect moving undistorted in an environment that is initially at rest. For pure Frank solutions, this has been computed in (*19*) for gliding undistorted disclinations. For $\gamma_2 = -\gamma_1$, the force fields $\mathbf{f}^{\pm} = \mathrm{div}\,\mathbf{T}^{\pm}$ created by moving $s = \pm\frac{1}{2}$ disclinations are

$$\mathbf{f}^{+} \propto \frac{1}{r^2}\Big[2(\cos\vartheta - \cos 2\vartheta)\,\mathbf{e}_r + (2\sin\vartheta - \sin 2\vartheta)\,\mathbf{e}_\vartheta\Big] \tag{51}$$

and

$$\begin{aligned} \mathbf{f}^{-} \propto \frac{1}{r^2}\Big[&2(2\cos 4\vartheta - \cos 2\vartheta - \cos\vartheta)\,\mathbf{e}_r. \\ &+ (\sin 4\vartheta - \sin 2\vartheta - 2\sin\vartheta)\,\mathbf{e}_\vartheta\Big], \end{aligned} \tag{52}$$

respectively. It is reasonable to assume that these expressions reflect the symmetry of the flow field that will eventually arise. Hence, we assume that $\mathbf{v} \propto \mathbf{f}^{\pm}$ and compute the integral of $\mathrm{tr}\mathbf{D}^2$ over the region outside the circle of radius r_e about the disclination centre for both $s = \pm\frac{1}{2}$, with the only purpose of estimating the ratio of the dissipations of $\mathcal{D}^-/\mathcal{D}^+$, which we assume also applies to the drag coefficients μ^- and μ^+. We thus arrive at $\mu^-/\mu^+ = 858/241 \approx 3.56$. Similar estimates can also be obtained for a generic topological charge s.

Repeating the same considerations for the disclination at $x = -a$, we find that the balances of forces for the two disclinations take the form

$$-2\pi\frac{K}{d}s^2 - \frac{\pi}{2}\gamma_1 su - \mu^+ v^+ = 0, \tag{53}$$

$$2\pi\frac{K}{d}s^2 - \frac{\pi}{2}\gamma_1 su - \mu^- v^- = 0, \tag{54}$$

where the superscripts + and – refer to the $+s$ disclination at $x = +a$ and the $-s$ disclination at $x = -a$, respectively. While the flow velocities $v^{\pm}$ at the two defects can be different, the reorientation speed u is the same for both disclinations.

3.4 Annihilation motion

We can now describe the motion of the two disclinations. If we denote by $x^{\pm}$ the position of the respective disclinations, their apparent velocities are then $\dot{x}^{\pm} = v^{\pm} \mp u$, where the flow velocities can be obtained directly from Equations (53) and (54). We express all lengths in terms of L and all times in terms of τ in (30) and obtain a coupled system of two ordinary differential equations:

$$\dot{x}^+ = -(\beta^+ s + 1)u - \frac{\beta^+ s^2}{x^+ - x^-}, \tag{55}$$

$$\dot{x}^- = -(\beta^- s - 1)u + \frac{\beta^- s^2}{x^+ - x^-}, \tag{56}$$

where we have set

$$\beta^{\pm} := \frac{\gamma_1 \pi}{2\mu^{\pm}}, \tag{57}$$

and u is a function of the defect distance $d = x^+ - x^-$,

$$u = -\frac{4}{d(d^2+4)\ln(r_c^2 d^2/(d^2+4))}, \tag{58}$$

see (31). For simplicity, we have retained the same symbols for the rescaled quantities.

These equations allow one to assess directly the asymmetry of the annihilation using the measure

$$\eta = \frac{\dot{x}^+ + \dot{x}^-}{\dot{x}^+ - \dot{x}^-} = \frac{s(\beta^+ + \beta^-)ud + s^2(\beta^+ - \beta^-)}{2ud + s(\beta^+ - \beta^-)ud + s^2(\beta^+ + \beta^-)}. \tag{59}$$

We note that $ud \to 0$ both for $d \to 0$ and $d \to \infty$, and so in these limits $\eta \to (\beta^+/\beta^- - 1)/(\beta^+/\beta^- + 1)$. Hence, the most important factor in determining the asymmetry in the annihilation is the ratio β^+/β^-.

To obtain quantitative results, we now focus on the case $s = \frac{1}{2}$ and consider a situation similar to that treated numerically in (5): we choose L = 100 nm, r_c = 2 nm comparable to the nematic correlation length, $\gamma_1 = 0.04$ Pas, $K = 10^{-11}$N, $\rho = 10^3\,\mathrm{kgm}^{-3}$, and $d_i = 150$ nm as the initial defect distance. With these parameters, $\tau = 10\,\mu$s. Figure 2 shows the resulting annihilation. Curve (a) shows the pure reorientational dynamics without flow, which corresponds to $\beta^{\pm} = 0$. To obtain curve (b), we used our estimate obtained above for the ratio $\beta^+/\beta^- = 3.56$, and we set $\beta^+ = 0.4$. This value for β^+, which is our only fitting parameter, was chosen so that the resulting annihilation time corresponds to that found in (5). Using these values for $\beta^{\pm}$, we have plotted in Figure 3 the anisotropy measure (59) as a function of the disclination distance d for different cut-off lengths. In both the limits for $d \to 0$ and $d \to \infty$, $\eta \approx 0.56$, but for $d \to 0$ the convergence to this value is very slow. The asymmetry is enhanced for larger cut-off lengths, but, for given L, it decreases for defect distances that are most relevant for the annihilation, that is, for $d < 2L$.

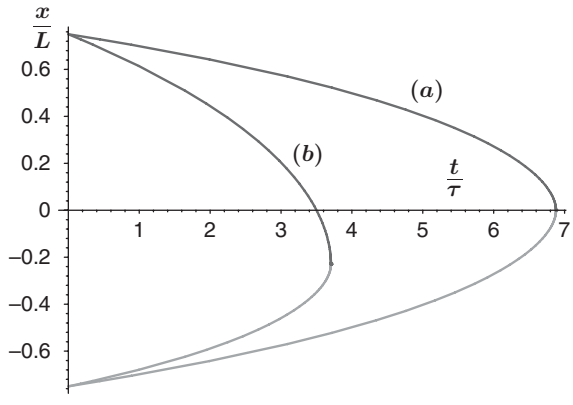

Figure 2. Defect annihilation (a) without flow and (b) with flow.

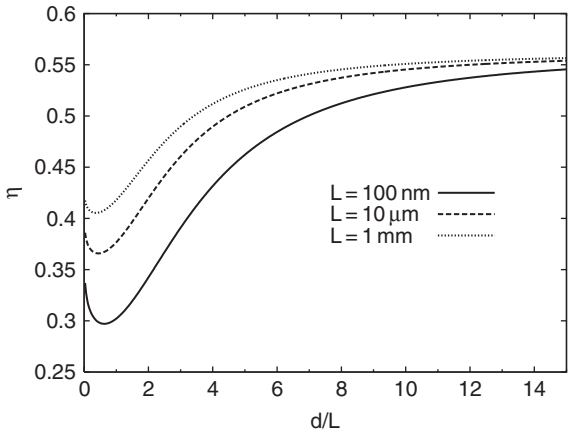

Figure 3. Asymmetry measure η as a function of the defect distance for different cut-off lengths.

4. Conclusions

We have proposed a phenomenological model for defect dynamics that accounts for both sources of defect motion: reorientation and fluid flow. The reorientation is treated in the usual way, neglecting flow. The induced flow is accounted for by requiring the contact forces on the defect to be balanced. We have distinguished and analysed three different types of force: an elastic force, a reorientational viscous force and a drag viscous force. We have applied the model to the annihilation of a pair of disclinations and found that it predicts correctly the asymmetry in this process. While for the small defect distances that have been analysed numerically in (*4–6*) the reorientational viscous forces contribute to the asymmetry, as they pull in the same direction, for larger defect distances the difference in the drag viscous force is the dominating factor. For intermediate distances, the asymmetry was shown to decrease, contrasting with the naive expectation that it remains almost unchanged for all distances.

Application of our model to point defects seems feasible: in that case both the elastic and the reorientational viscous force are proportional to the defect radius, as is Stokes's drag force on a sphere. An indication of how to compute the viscous drag force acting on point defects comes from the numerical results in (*20*): there, the drag on configurations with point defects was computed by employing Ericksen–Leslie theory. We expect the balance of forces on the defect to be again virtually independent of the defect radius.

References

(1) Ericksen, J.L. *Trans. Soc. Rheol.* **1961**, *5*, 23–34.
(2) Leslie, F.M. *Arch. Rational Mech. Anal.* **1968**, *28*, 265–283.
(3) Cladis, P.E.; van Saarloos, W.; Finn, P.L.; Kortan, A.R. *Phys. Rev. Lett.* **1987**, *58*, 222–225.
(4) Tóth, G.; Denniston, C.; Yeomans, J.M. *Phys. Rev. Lett.* **2002**, *88*, 105504.
(5) Svenšek, D.; Žumer, S. *Phys. Rev. E* **2002**, *66*, 021712.
(6) Svenšek, D.; Žumer, S. *Phys. Rev. Lett.* **2003**, *90*, 155501.
(7) Cladis, P.E.; Brand, H.R. *Physica A* **2003**, *326*, 322–332.
(8) Oswald, P.; Igneés-Mullol, J. *Phys. Rev. Lett.* **2005**, *95*, 027801.
(9) Blanc, C.; Svenšek, D.; Žumer, S.; Nobili, M. *Phys. Rev. Lett.* **2005**, *95*, 097802.
(10) Sonnet, A.M.; Virga, E.G. *Phys. Rev. E* **2001**, *64*, 031705.
(11) Ericksen, J.L. *Arch. Rat. Mech. Anal.* **1962**, *9*, 371–378.
(12) Gartland, E.C., Jr.; Sonnet, A.M.; Virga, E.G. *Continuum Mech. Thermodyn.* **2002**, *14*, 307–319.
(13) de Gennes, P.G.; Prost, J. *The Physics of Liquid Crystals*, 2nd edn; Clarendon Press: Oxford, 1993.
(14) Ryskin, G.; Kremenetsky, M. *Phys. Rev. Lett.* **1991**, *67*, 1574–1577.
(15) Denniston, C. *Phys. Rev. B* **1996**, *54*, 6272–6275.
(16) Leslie, F.M. *Continuum Mech. Thermodyn.* **1992**, *4*, 167–175.
(17) Guidone Peroli, G.; Virga, E.G. *Phys. Rev. E* **1996**, *54*, 5235–5241.
(18) Lamb, H. *Hydrodynamics*, 6th edn; Dover: New York, 1945.
(19) Sonnet, A.M. *Continuum Mech. Thermodyn.* **2005**, *17*, 287–295.
(20) Stark, H.; Ventzki, D.; Reichert, M. *J. Phys.: Condens. Matter* **2003**, *15*, S191–S196.